Journal of Materials Chemistry A

Self-supported branched Poly(ethyleneimine) Materials for CO2 Adsorption from Simulated Flue Gas

Journal:	*Journal of Materials Chemistry A*
Manuscript ID	TA-ART-05-2019-004662.R1
Article Type:	Paper
Date Submitted by the Author:	07-Jul-2019
Complete List of Authors:	Yoo, Chun-Jae; Georgia Institute of Technology, School of Chemical and Biomolecular Engineering Narayanan, Pavithra; Georgia Institute of Technology, School of Chemical and Biomolecular Engineering Jones, Christopher; Georgia Institute of Technology, School of Chemical and Biomolecular Engineering

SCHOLARONE™
Manuscripts

PAPER

Self-supported branched Poly(ethyleneimine) Materials for CO_2 Adsorption from Simulated Flue Gas

Received 00th January 20xx,
Accepted 00th January 20xx

DOI: 10.1039/x0xx00000x

Chun-Jae Yoo, Pavithra Narayanan, Christopher W. Jones

Self-supported, branched poly(ethylenimine) materials for CO_2 adsorption are prepared via an ice templating method. Crosslinking with poly(ethylene glycol) diglycidyl ether during the ice formation enables construction of a highly porous structure without utilization of freeze-drying. Depending on the amount of the crosslinker in the adsorbent, the sorbent family's CO_2 adsorption capacities and kinetics can be tuned, with sorbent materials offering optimum temperatures in the range of 25-75 °C. Different crosslinking temperatures used during preparation of adsorbents affect the physical structures of the adsorbents, which directly impact the sorption capacities and kinetics. An adsorbent prepared using liquid nitrogen is effective at 25 °C and offers an extremely high amine efficiency of 0.32 and capacity of 2.81 mol CO_2/kg sorbent, reaching 80% of its maximum capacity in only 18 min (10% CO_2 at 1 bar total pressure). This material's uptake rose to 5.5 mol CO_2/kg sorbent when the gas was at 65% relative humidity. The prepared adsorbent also presents stable recyclability over 50 dry adsorption-desorption cycles with only a minor loss of CO_2 capacity (4%). The CO_2 capacity over increasing cycles is estimated to converge at 95 % of its initial capacity according to a fitted exponential decay equation, making this material a promising new material for post-combustion CO2 capture.

Introduction

Of various emerging CO_2 adsorption materials, inorganic-organic hybrid materials (e.g., silica-supported amine adsorbents) are amongst the most efficient materials for CO_2 capture from relatively low CO_2 concentration sources such as flue gas (10-15%) and ambient air (0.04%, 400 ppm) via chemisorption.[1–6] In accordance with their physical and chemical features, these materials have been categorized into several classes;[7] Class 1: physical impregnation of polyamines (amine molecules or amine polymers) on a support, Class 2: covalent grafting of aminosilanes on a support, Class 3: covalent grafting of amine polymers on a support via in-situ polymerization, Class 4: combination of class 1 and class 2 features.[8]

Despite these differences in preparation methods, a common feature of these amine functionalized adsorbents is that a supporting material is an indispensable component to increase the potential amine contact area with CO_2 molecules in the target gas. Unsupported amine molecules have been repeatedly shown to have low CO_2 capacities and slow adsorption kinetics due to hindered mass transport associated with their low surface area.[9–11] In this context, highly porous powder type support materials (e.g., silica,[10,12–20] alumina,[21–23] carbon[24] or polymer[25,26]) have been primarily utilized to enhance the CO_2 uptake by increasing the number of accessible amine groups on the high surface area support.

Solids prepared by lyophilization (freeze-drying) are one class of materials that have been used to enhance the porosity of solid materials in applications targeting adsorption. One way to make such materials is to employ an aqueous solution containing a solid support component (e.g., graphene oxide, cellulose or carbon nanotubes)[27–29] and amine molecules and freeze it at a given temperature, whereby the formed ice crystals are then sublimed under reduced pressure. The ice acts as a scaffold or porogen, which generates a highly porous structure after sublimation. In past work amine molecules were most often impregnated or grafted on the surface of a previously generated porous structure to make solid composites.

To achieve a highly porous structure in the powder adsorbents, quite often, relatively expensive surfactants are used in academic studies, which is likely too expensive for deployment at scale. Similarly, aminosilanes are also quite expensive in many cases, making large scale deployment of sorbents built from them potentially challenging. For these reasons, rapid deployment of amine sorbents in emerging separations such as direct air capture (DAC) might be best achieved using sorbents employing conventional ingredients with modest costs that are already produced on a large scale. To this end, monolith[30–32] or hollow fiber[33] supported adsorbents prepared by impregnating them with amine solutions made with polymers already produced at scale, such as poly(ethyleneimine) (PEI), may be more suitable platforms for practical application of CO_2 adsorption. However, if the amine molecules themselves could similarly adsorb CO_2 without

[a] School of Chemical & Biomolecular Engineering, Georgia Institute of Technology, 311 Ferst Drive NW Atlanta Georgia 30332 United States, Email: cjones@chbe.gatech.edu

Electronic Supplementary Information (ESI) available: [details of any supplementary information available should be included here]. See DOI: 10.1039/x0xx00000x

utilization of an added support, which adds unwanted sensible heat load in addition to the desired high surface area, one would have a new, promising sorption material for practical application.

Several studies have introduced porous polymer adsorbents[34–39] that adsorb CO_2 molecules without support materials. However, in many such reports, the free amine groups of the monomers are transformed into less basic groups that are much less efficient at CO_2 adsorption such as imine, amide, triazole or melamine groups during the polymerization. The amine affinity of these groups toward CO_2 molecules is much lower than primary or secondary amines, which are often used for post-combustion capture or DAC applications. As a result, the CO_2 capacities for those polymers at dilute CO_2 concentrations are relatively low compared with the conventional supported amine adsorbents. In another approach to prepare self-supported CO_2 adsorbents, Hwang et al.[40] reported the use of partially crosslinked, branched poly(ethyleneimine) (b-PEI) with glutaraldehyde via a water-in-oil emulsification method. After the crosslinking, the liquid phase of neat b-PEI was transformed into a solid phase in the form of a spherical shaped bead (0.2-2 µm). The highest CO_2 capacity of the bead was 2.18 mmol CO_2/g under 1 bar CO_2 pressure at 75 °C, with exposure for 3h. Xu et al.,[41] synthesized non-porous PEI hydrogel beads (1200-1400 µm) for CO_2 absorption, where the b-PEI was crosslinked with epichlorohydrin via sedimentation polymerization in canular oil. The prepared hydrogel beads were pre-wet with various water contents and the measured maximum CO_2 absorption was 1.36 mmol CO_2/g under 2 bars CO_2 at 25 °C for 1 h. Note that while both of these uptake capacities initially appear strong, they are obtained at high CO_2 partial pressures, not at the relevant pressures for DAC or post-combustion capture, which are orders of magnitude lower.

In this work, we introduce a new type of self-supported PEI adsorbent that can be prepared by a simple ice-templating method. The conventional ice-templating method requires a sequential freeze-drying process under reduced pressure.[42–45] For preparation of this adsorbent, however, to simplify the process, poly(ethylene glycol) diglycidyl ether is used as a crosslinking agent and the b-PEI is crosslinked in aqueous solution while the solution is being frozen. This allows a highly porous structure to be maintained after the thawing process instead of using a freeze-drying process. The CO_2 capacity and stability of the self-supported PEI adsorbents were then explored under simulated flue gas conditions (dry or wet) to evaluate the potential of the material as a new, inorganic support-free CO_2 sorption material.

Experimental

Materials

The 50 wt.% branched poly(ethyleneimine) (b-PEI, (M_n 60,000 by GPC, M_w 750,000 by LS)) in aqueous solution (primary/secondary/tertiary amine = 40:40:20) (Figure S1), b-PEI (Mn ~600 GPC, Mw ~800 by LS) and poly(ethylene glycol) diglycidyl ether (PEGDGE, Mn: 500), Poly(ethylene glycol)-block-poly-(propylene glycol)-block-poly(ethylene glycol) (Pluronic P123, Mn ~5800), tetraethyl orthosilicate (TEOS) were purchased from Sigma Aldrich and used without further purification. Hydrochloric acid (HCl, 37%) and methanol were purchased from EMD.

Preparation of crosslinked b-PEI adsorbent

The crosslinking of b-PEI was carried out by following the method of S. Chatterjee *et al*., who deployed cross-linked PEI sponges for separation of liquid mixtures[46] First, the 50 wt.% b-PEI (M_n 60,000 by GPC, M_w 750,000 by LS) aqueous solution was diluted to a 10 wt.% b-PEI stock solution by adding DI water. Then, 1.6 g of the stock solution (160 mg of b-PEI) and the PEGDGE (50 - 400 µL) were mixed in a 8 mL of glass vial with a vortex mixer (500 rpm) for 5 s. The mixture was immediately transferred to the freezer (-10 °C) and stored for two days. For a liquid nitrogen treated sample, the mixture was instantly frozen with liquid nitrogen by immersing the vial into the liquid nitrogen bath, which was then stored in the freezer for two days. For a room temperature treated sample, the mixture was stored at room temperature for two days without any treatment. The prepared frozen samples were thawed at room temperature, and the vial was carefully broken to collect the samples. The samples were washed with methanol and dried under vacuum overnight at 60 °C. The prepared samples were labeled as EX-Y, where X represents the volume of PEGDGE (50 - 400), and Y represents the curing conditions (room temperature (RT), freezer (FZ) or liquid nitrogen (LN_2).

Preparation of b-PEI functionalized SBA-15

For the comparation with crosslinked b-PEI adsorbents, 40 wt.% b-PEI impregnated SBA-15 was prepared as reported in the literature.[16] Briefly, 40 mg of b-PEI (Mn ~600 GPC, Mw ~800 by LS) and 60 mg of SBA-15 were stirred in 20 mL of methanol for 2 h, then the solvent was evaporated by rotary evaporator. The powder was further dried at 60 °C overnight under vacuum.

Characterization

For the solution-state nuclear magnetic resonance (NMR) measurements (Advance III 400 MHz, Bruker) the 50 wt.% b-PEI was concentrated with rotary evaporated and dissolved in MeOD solvent. For quantitative analysis of the ratios of primary, secondary and tertiary amines in the b-PEI, ^{13}C NMR spectra were recorded with 10 s relaxation time for 512 scans. For the scanning electron microscopy (SEM) analysis, samples placed on carbon tape attached to a sample holder were gold-coated with a gold sputterer (Q150T ES, Quorum) for 30 s. The SEM images were taken at 3 kV of voltage and 10 A of ion current (SU8010, Hitachi). The average pore size of the material was estimated from more than 30 pores by using an imaging program (Digimizer). The elemental compositions (C and N) of the samples were measured by combustion using an automatic analyzer, which was conducted at Atlantic Microlab (Norcross, GA). For the FTIR measurements, samples placed on diamond

This journal is © The Royal Society of Chemistry 20xx

Please do not adjust margins

crystal of the ATR accessory (Smart iTR, Thermo Scientific) equipped with IR spectrometer (Nicolet iS10, Thermo Scientific). The IR signals were recorded with 64 scans at a resolution of 4 cm^{-1}.

CO_2 capacity measurements

CO_2 adsorption capacities for the samples under dry conditions were measured by TGA (Q500, TA Instruments). Each sample was pre-treated under He flow at 110 °C for 2 h and subsequently equilibrated at the adsorption temperature (25, 45, 55, 65 and 75°C). Then, the samples were exposed to 90 mL/min of 10% CO_2/He gas for 3 h or 12 h. For the measurement of CO_2 capacity under humid conditions, 0.15 - 0.2 g of sample was loaded in a ¼ inch diameter glass tube, which was pre-treated under N_2 flow (50 mL/min) at 110 °C for 2 h. Then, the sample was saturated with humid nitrogen (Rh= 65%) flow at 25 °C, and the gas flow was changed to humidified 10% CO_2/10% He/N_2 gas flow (12 or 20 mL/min, RH= 65%), where the He was used as a tracer. The outlet gas composition was recorded via mass spectroscopy (ThermoStar GSD 320 T, Pfeiffer Vacuum Inc.). The CO_2 adsorption-desorption cycle tests were conducted by TGA. Firstly, the sample was dried under He flow (90 mL/min) at 100 °C for 10 min for desorption, and the temperature was equilibrated at 45 °C for CO_2 adsorption with 10% CO_2/He gas flow (90 mL/min) for 20 min. This adsorption-desorption sequence was cycled 50 times.

Results

Self-supported PEI adsorbents

Self-supported PEI adsorbents were prepared by an ice-templating method as described in Scheme 1. As the water molecules are frozen, the B-PEI is crosslinked with PEGDGE, which generates a compressible scaffold structure between the ice crystals. The shape of the adsorbent can be easily controlled by the shape of the mold, if shaped structures are sought. In this study, the crosslinked PEI adsorbent was formed in a cylindrical shape because a glass vial was used as the mold. The cylindrical structure of the sorbent material was well maintained even during the breakage of the vial needed to recover the adsorbents, as well as through the drying process, as shown in Figure S2. However, the size of the adsorbent was slightly reduced compared to the wet adsorbent, from which one can infer that the extended carbon backbone of the crosslinked PEI in water shrank while the thawed water was evaporated. The degree of shrinkage of the adsorbent varied depending on the content of the crosslinker, PEGDGE, in the adsorbent. If the volume of added PEGDGE was less than 50 μL (based on the 160 mg of PEI), the cylindrical shape of the adsorbent was not maintained, and the material became an irregular, flat structure. It seems that the porous structure of the adsorbent

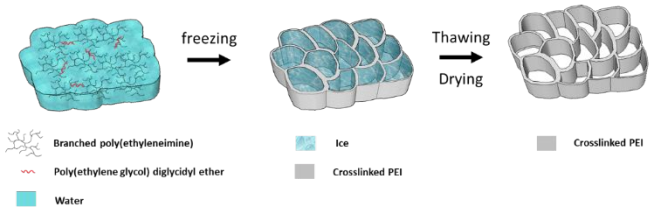

Scheme 1. Schematic synthesis of the self-supported PEI adsorbent.

Table 1. The weights of PEI and volumes of PEGDGE of samples and their amine loadings.

Samples	PEI weight (mg) (N mmol)[a]	PEGDGE volume (μL) (epoxide mmol)[b]	Amine loading (mmol N/$g_{adsorbent}$)[a]
b-PEI (60 kda)	n.a.	n.a.	25.3
E50-FZ		50 (0.2)	16.6
E100-FZ		100 (0.4)	12.6
E150-FZ		150 (0.7)	11.0
E200-FZ	160 (4.1)		8.2
E200-RT		200 (0.9)	8.8
E200-LN_2			8.8
E400-FZ		400 (1.8)	5.8

[a] measured by elemental analysis, [b] theoretical value (mol of PEGDGE x 2)

provided by ice crystals collapsed in such cases after the evaporation of water because the added volume of PEGDGE was not enough to prevent the collapse. The collapsed structure rebounded back to the original, cylindrical structure after adding several water drops, as shown in Video S1.

The added weight of b-PEI and the volume of PEGDGE for the synthesis of the array of adsorbents are summarized in Table 1. The overall amine loading (a combination of primary, secondary and tertiary amines) for the adsorbents was measured by elemental analysis, and the results are also shown in Table 1. As the composition of the PEGDGE in the adsorbent increases, the overall amine loading decreases because a larger amount of PEGDGE was crosslinked with the same amount of PEI.

The possible chemical reactions between the b-PEI and PEGDGE are shown in Scheme 1. The reaction of a primary amine of b-PEI with an epoxide of PEGDGE produces a secondary amine and a secondary alcohol (1). The secondary amine of the product from the reaction (1) can sequentially react with another epoxide to generate a tertiary amine and another secondary alcohol (2) or similarly, a secondary amine of PEI can react with epoxide to yield tertiary amine and secondary alcohol (2'). Depending on the epoxide to amine ratio, the secondary alcohol may additionally react with epoxide (esterification reaction) which produces ether linkages (3). However, this reaction would be limited in our system because a high curing temperature is required for the efficient

This journal is © The Royal Society of Chemistry 20xx

Please do not adjust margins

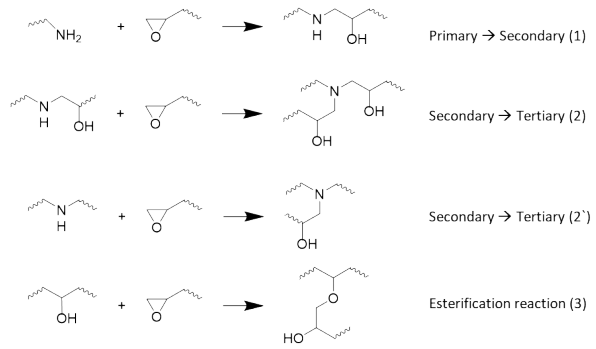

Scheme 2. The possible chemical reactions between the amines of the b-PEI and the epoxide of the PEGDGE

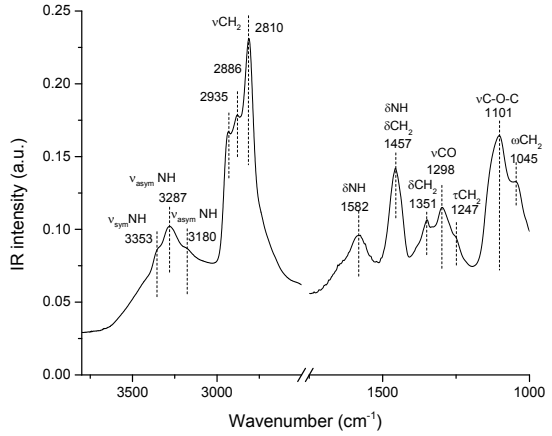

Figure 1. FTIR spectra of the crosslinked PEI adsorbent (E100-FZ)

condensation of water and the reaction rate is quite low.[47,48] Furthermore, since the epoxide to amine ratio in our system is extremely low (0.06 - 0.45) and the epoxide reaction rate with primary amines is sufficiently faster than with secondary amines,[48] most of the epoxides of PEGDGE would primarily react with the primary amines, reacting with secondary amines only to a small extent, during the crosslinking procedure at low temperature.

The FTIR spectrum of the self-supported adsorbent, E100-FZ, is presented in Figure 1. All the adsorbents showed similar peaks without any distinguishable differences. The bands at 3353-3180 cm^{-1} are assigned to the asymmetric or symmetric stretching of primary or secondary amine groups. The three peaks at 2935-2810 cm^{-1} are attribute to the stretching vibrations of methylene groups in the adsorbent. The bending vibration peak at 1582 and 1457 cm^{-1} (δNH) are associated with N-H bond.[49,50] The band at 1457 cm^{-1} also can be assigned to bending vibrations of methylene groups (δCH).[51] The other C-H vibration modes (bending,[52] twisting,[51] wagging[53]) were also observed at 1351, 1247, 1045 cm^{-1}. The stretching vibration of C-O (νCO)[54] and C-O-C (νC-O-C)[55,56] of the PEGDGE appeared at 1298 and 1101 cm^{-1}, respectively.

To ascertain the physical morphologies of the crosslinked PEI adsorbents, SEM images of the adsorbents were taken (Figure 2). In general, neat B-PEI and PEGDGE are in the liquid phase at room temperature, but once the PEI is crosslinked with PEGDGE, the adsorbents transform into a solid phase, as shown in Figure 2. During the crosslinking process at low temperature (-10 °C for freezer, -196 °C for LN_2 treatment), ice crystal fragments are formed, which occupy space between the polymer chains. Then, the volume of the ice is transformed into a macroporous structure when the ice crystals are thawed and removed. Due to the macroporous structure or flexibility of the materials, the surface areas and the pore volumes of the adsorbents were not able to be measured with the conventional, cryogenic nitrogen physisorption method. However, a noticeable trend in the average pore size of the adsorbents was observed depending on the crosslinker content

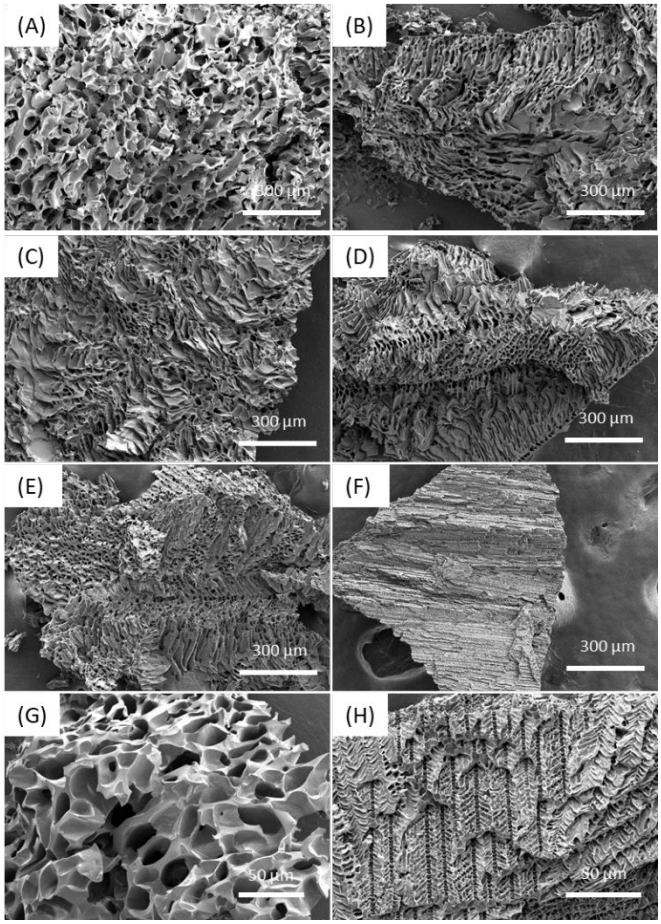

Figure 2. SEM images of crosslinked PEI adsorbents. (A) E50-FZ, (B) E100-FZ, (C) E150-FZ, (D) E200-FZ, (E) E400-FZ, (F) E200-LN2, (G) magnified E200-FZ (H) magnified E200-LN_2

in the adsorbents (Figure S3). For the E50-FZ adsorbent, the average pore size was relatively larger (41±9 µm) than for the other adsorbents containing higher crosslinker contents, and the irregular shape of the pores was interconnected in the adsorbents (Figure 2A). As the content of the PEGDGE in the adsorbent increases, the average pore size was slightly reduced (Figure S3, E100-FZ: 21±5 µm, E150-FZ: 15±3 µm, E200-FZ: 13±3 µm, E400-FZ: 11±2µm), and the macropore structures became more ordered, with a combination of lamellar and pillared structures (Figure 2B-E and G). Interestingly, when the adsorbent was prepared with liquid nitrogen treatment (E200-LN_2), the pore size was dramatically reduced to 3±0.5 µm and a

This journal is © The Royal Society of Chemistry 20xx

Please do not adjust margins

highly ordered pore structure was observed (Figure 2F and H). Depending on the freezing conditions, the morphology and growth rate of the ice crystals are varied.[57–59] When the freezing temperature is relatively high (-10 °C), the ice crystal grows slowly, which increases the ice crystal size. During the freezing, the slowly growing ice crystals push out the mixture of PEI and PEGDGE, which causes formation of thick walls from the mixture of the PEI and PEGDGE. On the other hand, a number of ice nuclei are nucleated and simultaneously grow fast at -196 °C (liquid nitrogen temperature) and the mixture of the PEI and PEGDGE becomes trapped between small ice crystals in a short timeframe, as depicted in Figure S4.[60–63] When the b-PEI was crosslinked with PEGDGE at room temperature (E200-RT), a porous structure was not observed.

The CO_2 capacities of the self-supported PEI adsorbents under dry 10% CO_2 conditions were measured for 3 h at various sorption temperatures. Since each sample contains different amine loadings, the obtained CO_2 uptake values were also normalized by the amine loadings, which allows for a normalized comparison among the prepared adsorbents in terms of amine efficiencies (amine efficiency = adsorbed CO_2 mmol/N mmol in adsorbent). The overall CO_2 uptakes and amine efficiencies of the adsorbents at the various temperature are presented in Figure 3. The E50-FZ material adsorbed 0.25 mmol CO_2/g (amine efficiency: 0.01) at 25 °C, however, the CO_2 capacity (up to 3.0 mmol CO_2/g at 75 °C) and amine efficiency (up to 0.18 at 75 °C) of the sample were improved as the adsorption temperature increased. This trend of improved performance at elevated temperatures has been reported in several studies that have used conventional silica supported PEI materials.[9,16,64–67] In general, CO_2 adsorption with supported PEI adsorbents has been explained from a combination of thermodynamic and kinetic perspectives. Thermodynamically, CO_2 adsorption is favored at lower temperature because the adsorption phenomenon is an exothermic process. However, the mobility of the polymer chains of the PEI increases with increasing temperature, which improves the kinetics of access of CO_2 to the amine groups in materials with high density polymer domains, some of which may have previously been not easily accessed at low temperatures. Thus, the kinetic effects can be the dominant factor vs. the thermodynamic effect for CO_2 uptake behavior of the adsorbent, depending on the thickness of the PEI film or domain. From this context, the maximum CO_2 capacity of the E50-FZ adsorbent at 75 °C can be rationalized.

For the E100/150-FZ adsorbents, the maximum CO_2 capacities (2.75 and 2.0 mmol CO_2/g, respectively) and amine efficiencies (0.20 and 0.19, respectively) were observed between 45–55 °C. For the E200/400-FZ adsorbents, the maximum CO_2 capacities (2.02 and 1.10 mmol CO_2/g, respectively) and amine efficiencies (0.21 and 0.18, respectively) were obtained at the lowest tested temperature, 25°C, such that thermodynamics dominantly govern the CO_2 capacities on the E200/400-FZ adsorbents.

As the degree of crosslinking of PEI by PEGDGE increases, the temperature for the maximum CO_2 capacity is lowered, which indicates that a higher degree of crosslinking may effectively prevent an aggregation of the polymer chains even at the lower

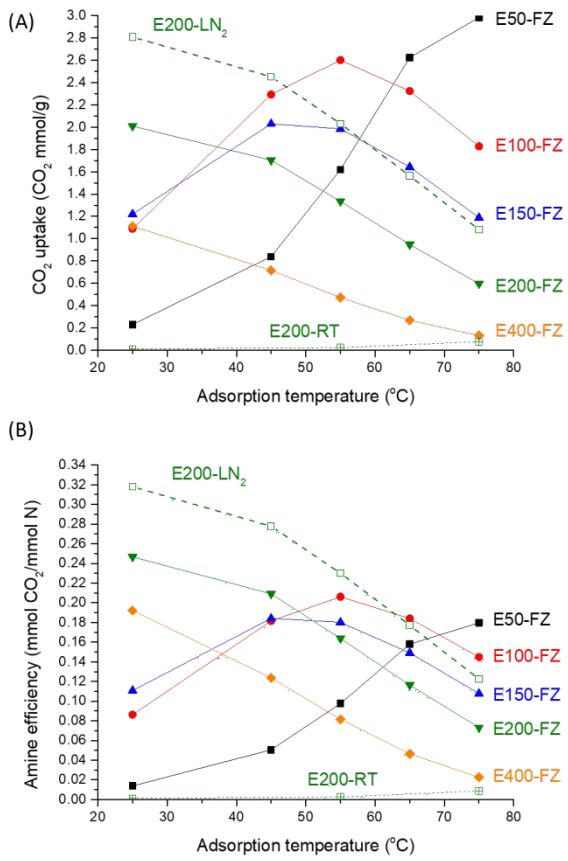

Figure 3. (A) CO_2 uptake (10% CO_2/balance He, 3 h) and (B) amine efficiency of the crosslinked PEI adsorbents on various temperatures (25, 45, 55, 65, 75 °C).

adsorption temperatures (i.e., 25 °C). The non-crosslinked PEI chains may become more aggregated, or macropores of the adsorbents may collapse when the ice crystal template is removed, which likely caused the decreased amine efficiency at 25 °C (E50-FZ: 0.01, E100-FZ: 0.08, E150-FZ: 0.11, E-200-FZ: 0.25, Figure 3B). In the case of E400-FZ, the primary and secondary amines of the PEI are further reacted with epoxy groups to yield less active amines, secondary or tertiary amines, which might lead to a reduced amine efficiency (E400-FZ: 0.19) at 25 °C.

These proposed aggregations of the polymer chains and collapse of macropores in the adsorbents may affect the porosity of the adsorbents. Since the water content in the frozen sample was identical for all the adsorbents, when the pore size decreased, as presented in Figure 2 and S3, the surface area of the adsorbents increased, with the average wall thickness decreasing, which may lead to a higher amine efficiency at 25 °C. However, when the measurement temperature increased, the morphology of adsorbents may change further, and it might be difficult to explain the CO_2 uptake by solely analysis of the wall thickness and porosity of the adsorbents.

Other than the crosslinker to b-PEI ratio in the adsorbent, the curing temperature also influences the CO_2 sorption capacity. The adsorbent (E200-RT) crosslinked at room temperature displayed the lowest CO_2 capacity at all the temperatures tested

Please do not adjust margins

due to its nonporous structure and limited amount of accessible amine sites for CO_2 adsorption. Even though the E200-RT was as highly crosslinked as E200-FZ, CO_2 molecules cannot easily contact the amine groups located inside the nonporous sample. The CO_2 molecules may be adsorbed by only the external surface area of E200-RT, while the CO_2 molecules would have higher accessibility toward amine groups located inside of the E200-FZ material due to the macropores formed by ice crystals. When the adsorbent was pre-frozen in liquid nitrogen before being stored in the freezer, the CO_2 capacity of the adsorbent (E200-LN_2) markedly improved (~30 %) compared with the E200-FZ adsorbent. The pore size and wall thickness of the E200-LN_2 material were found to be much thinner than for the E200-FZ adsorbent, as shown in Figures 2G and H, which allows for more amine groups of the adsorbents (E200-LN_2) to be easily accessed by CO_2. The obtained amine efficiency (0.32) of the E200-LN_2 at 25 °C is the highest value among silica supported PEI adsorbents under the same conditions (10% CO_2 concentration at 25 °C) reported so far, to our best knowledge. The summarized results are shown in Table S1 or Figure S5. Most of the studies that utilized PEI based adsorbents have focused on higher adsorption temperature (> 75 °C) because the maximum CO_2 capacities for such material are normally observed at such elevated temperature. On the other hand, these crosslinked adsorbents can be tuned to achieve higher CO_2 capacity or amine efficiency at any targeted adsorption temperature by controlling the crosslinker content, presenting an advantage for this class of materials.

To evaluate the effect of humidity on the self-supported adsorbents, breakthrough experiments were conducted at a RH 65%, at 25 °C. For a validation of the experiment, the measured CO_2 capacity under dry conditions from the breakthrough device was compared with the value from the gravimetric method, and it was found that the CO_2 uptakes from both methods were comparable (Table 2). The CO_2 capacity of the E200-FZ adsorbent under humid conditions was 3.36 mmol CO_2/g, which was 64% higher compared with the CO_2 capacity under dry conditions. Even more significant, the E200-LN_2 adsorbents showed 103 % improved CO_2 capacity against the standard, dry conditions. Considering that the volume of the dried self-supported PEI adsorbents generally rebounded back to their original size when it was rewet, as shown in Video S1, the expansion of the volume of the adsorbent under humid conditions may increase the number of accessible amine sites for CO_2 adsorption. Another possibility is that amine efficiency of the adsorbents increases under humid conditions due a change in the population of adsorbed CO_2 species amongst the known forms (alkylammonium carbamate, alkylammonium bicarbonate, carbamic acid).[68–71] It is known that CO_2 molecules can be captured by one primary or secondary amine group under humid conditions (maximum theoretical amine efficiency =1) while the maximum theoretical amine efficiency under dry conditions is 0.5.[72–75] Thus, the enhanced CO_2 capacities of the self-supported adsorbents under humid conditions might be derived by a combination of an increased number of amine sites and higher amine efficiency.

The adsorption rate is one of the most important elements in evaluating the performance of an adsorbent, as practical application of the materials requires rapid cycling to limit solid sorbent inventories in the plant. Thus, in practical applications, the sorbent material needs to demonstrate fast and stable adsorption-desorption cycles in a short time frame. To evaluate the kinetic sorption properties of the adsorbents, the CO_2 capacity of each adsorbent at 25 °C was normalized (Figure 4A), and the maximum CO_2 capacity and adsorption half-time of each adsorbent is shown in Figure 4B. As the crosslinker ratio to PEI increases, the adsorption half-time is intensely reduced as follows, 184 min (E50-FZ) → 129 min (E100-FZ) → 117 min (E150-FZ)→ 25 min (E200-FZ) → 3 min (E400-FZ). The E200-LN_2

Samples	Dry CO_2 capacity [a]	Dry CO_2 capacity [b]	Humid CO_2 capacity[b] (RH 65%)
E200-FZ	2.01 mmol CO_2/g	2.05 mmol CO_2/g	3.36 mmol CO_2/g
E200-LN_2	2.81 mmol CO_2/g	2.70 mmol CO_2/g	5.50 mmol CO_2/g

Table 2. Equilibrated CO_2 uptakes of self-supported PEI adsorbents under dry and humid (RH: 65%) conditions

[a] measured by TGA equipment at 25 °C, [b] measured by breakthrough equipment at 25 °C

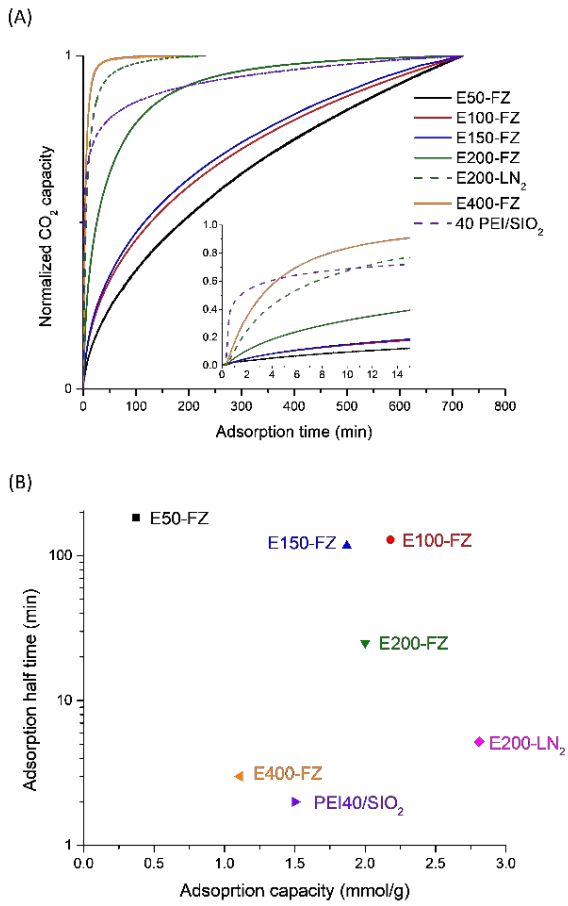

This journal is © The Royal Society of Chemistry 20xx

Please do not adjust margins

Figure 4. (A) Normalized CO_2 capacity and (B) CO_2 adsorption capacity and adsorption half time of the self-supported PEI adsorbents at 25 °C.

showed higher CO_2 capacity (2.8 mmol CO2/g) and faster adsorption half time (5 min) than the E200-FZ material. As a benchmark material, the data for a 40wt.% PEI/SiO_2 material are also shown in Figure 4. The PEI40/SiO_2 reached 50% of its maximum capacity in the shortest time (2 min), but the CO_2 adsorption rate was noticeably reduced after the adsorption half time. In contrast, while it takes 49 mins for PEI40/SiO_2 to reach 80% of its maximum CO_2 capacity, E400-FZ and E200-LN_2 reached 80% of their maximum capacities in 9 min and 18 min, respectively. Thus, while these self-supported b-PEI sorbents may have slower initial uptake rates, a larger fraction of their total capacity may be accessible in short cycle times compared to conventional amine adsorbents.

We also investigated the cyclic stability of the adsorbent (E200-LN_2) over 50 cycles of adsorption (10% CO_2 in He, 45 °C for 20 min) and desorption (He, 100 °C for 10 min). The fresh sample adsorbed 2.28 mmol CO_2/g and the 50 times cycled sample adsorbed 2.17 mmol CO_2/g, which was 95.6% of CO_2 capacity of fresh adsorbent. More specifically, the major loss (3.5%) was observed during the first 20 adsorption-desorption cycles, and the CO_2 capacity slightly decreased (0.9%) for the last 30 cycles. Several research groups have reported that the amine groups of PEI are thermally degraded during multiple temperature swing cycles under dry conditions, where the CO_2 capacity was significantly reduced due to the loss of amine groups via urea formation at high temperature (>105 °C).[76,77] However, in some recent work, this CO_2-induced degradation of PEI via urea formation has been effectively mitigated by epoxidation of the PEI.[78] Under an identical set of cycle conditions, the epoxy-treated PEI/SiO_2 adsorbent maintained its CO_2 capacity over 50 cycles, but the PEI/SiO_2 adsorbent lost 45% of its CO_2 capacity. The suppressed formation of urea on the epoxidized PEI was explained in their work due to elimination of primary amines of the PEI via epoxidation, which effectively suppressed the formation of open-chain urea that favorably occurs on primary amine. Additionally, the ring opened bulky 2-ethyl-hydroxyethyl groups (-$CH_2CH(C_2H_5)OH$) could sterically hinder the formation of urea in their work. Recently, epoxide modified linear polyamines (TEPA, PEHA) were also reported as stable amine adsorbents against urea formation.[79]

Considering that main reaction in crosslinking of the self-supported PEI adsorbent is also epoxidation of the amines of the b-PEI to yield 2-ethyl-hydroxyethyl groups (-$CH_2CH(C_2H_5)OH$), as shown in Scheme 2, the stable recyclability of the adsorbents is very likely due to suppressed urea formation. Significant evidence of urea formation on the 50 times recycled adsorbent was not observed from an IR investigation. Figure S6 shows the normalized CO_2 capacity over 50 cycles and a fitted exponential decay equation describing the capacity loss, $y = 4.4 \cdot \exp(-x/11.8) + 95.6$, where y is the CO_2 capacity after x cycles. This suggests that CO_2 capacity will be converged to ~95.5 % of CO_2 capacity of the fresh adsorbent at a steady state.

Figure 5. Cycle of CO_2 adsorption-desorption for P160-E200-FZ. Adsorption

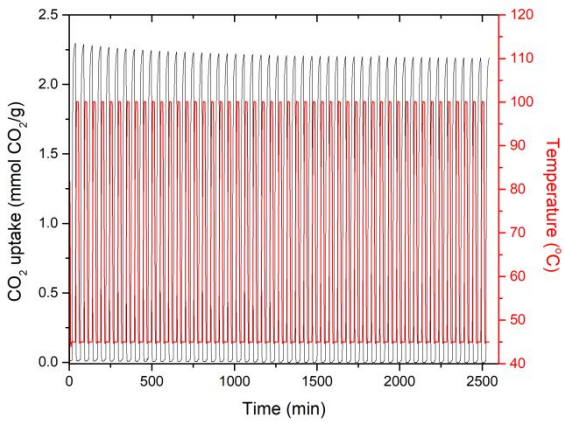

conditions (10% CO_2 in He at 45°C for 20 min), Desorption conditions (He at 100°C for 10 min)

Conclusions

Self-supported PEI adsorbents were prepared by an ice templating method where the b-PEI was crosslinked with various amounts of PEGDGE. Instead of utilization of a conventional freeze-drying process, highly porous adsorbents were generated after a simple thawing process. As the crosslinker content in the adsorbent increased, the average diameter of macropores of the adsorbent decreased, and the adsorption temperature for the maximum CO_2 capacity decreased from 75 °C (E50-FZ) to 25 °C (E400-FZ). Initial sorbent synthesis temperatures (25 °C, -10 °C or -196 °C) also remarkably affected the porous structure and CO_2 adsorption properties of the adsorbents. While the E200-RT sample with a non-porous structure presented extremely low CO_2 capacity at all the temperatures tested, a highly ordered pore structure was observed from E200-LN_2, which significantly improved the CO_2 sorption capacity and kinetics. Furthermore, the swollen property of the wet adsorbents allowed for increased CO_2 capacity under humid gas conditions. Compared with conventional supported PEI adsorbents, the self-supported b-PEI adsorbents exhibited similar or even higher amine efficiencies at certain temperatures, demonstrating that CO_2 adsorbents using amine molecules do not need to be loaded on porous support materials to generate higher CO_2 capacities. Furthermore, the prepared adsorbents showed an outstanding adsorption-desorption stability over 50 cycles with fast kinetics. In this study, the self-supported b-PEI material showed multiple aspects of promising CO_2 adsorbents in terms of (i) good CO_2 capacity, (ii) rapid kinetics, and (iii) improved stability over conventional supported amine adsorbents. Additionally, the material can be prepared by a simple and potentially economical method and can likely be easily molded into any shape. Most importantly, use of additional support material is not required to prepare the adsorbent. Considering these factors, the results from this study may contribute to development of new types of CO_2 sorption materials that

Please do not adjust margins

improve the stability and reduce the cost of amine-based CO_2 sorbents.

Conflicts of interest

There are no conflicts to declare.

Acknowledgements

Funding for this work was provided in part by UNCAGE-ME, an Energy Frontier Research Center funded by the U.S. Department of Energy, Office of Science, Basic Energy Sciences under award no. DE-SC0012577 and in part by the Love Family Professorship and William R. McLain Chair at Georgia Tech.

References

1 S. Choi, J. H. Drese and C. W. Jones, *ChemSusChem*, 2009, **2**, 796–854.
2 E. S. Sanz-Perez, C. R. Murdock, S. A. Didas and C. W. Jones, *Chem. Rev.*, 2016, **116**, 11840–11876.
3 H. A. Patel, J. Byun and C. T. Yavuz, *ChemSusChem*, 2017, **10**, 1303–1317.
4 A. Samanta, A. Zhao, G. K. H. Shimizu, P. Sarkar and R. Gupta, *Ind. Eng. Chem. Res.*, 2012, **51**, 1438–1463.
5 B. Dutcher, M. Fan and A. G. Russell, *ACS Appl. Mater. Interfaces*, 2015, **7**, 2137–2148.
6 A. Sayari, Y. Belmabkhout and R. Serna-Guerrero, *Chem. Eng. J.*, 2011, **171**, 760–774.
7 P. Bollini, S. A. Didas and C. W. Jones, *J. Mater. Chem.*, 2011, **21**, 15100–15120.
8 W. C. Wilfong, B. W. Kail, C. W. Jones, C. Pacheco and M. L. Gray, *ACS Appl. Mater. Interfaces*, 2016, **8**, 12780–12791.
9 X. Xu, C. Song, J. M. Andresen, B. G. Miller and A. W. Scaroni, *Energy and Fuels*, 2002, **16**, 1463–1469.
10 W.-J. Son, J.-S. Choi and W.-S. Ahn, *Microporous Mesoporous Mater.*, 2008, **113**, 31–40.
11 X. Xu, C. Song, J. M. Andresen, B. G. Miller and A. W. Scaroni, *Microporous Mesoporous Mater.*, 2003, **62**, 29–45.
12 N. Hiyoshi, K. Yogo and T. Yashima, *Microporous Mesoporous Mater.*, 2005, **84**, 357–365.
13 X. Yan, S. Komarneni and Z. Yan, *J. Colloid Interface Sci.*, 2013, **390**, 217–24.
14 R. Sanz, G. Calleja, A. Arencibia and E. S. Sanz-Pérez, *Microporous Mesoporous Mater.*, 2012, **158**, 309–317.
15 C.-J. Yoo, L.-C. Lee and C. W. Jones, *Langmuir*, 2015, **31**, 13350–13360.
16 R. Sanz, G. Calleja, A. Arencibia and E. S. Sanz-Pérez, *Appl. Surf. Sci.*, 2010, **256**, 5323–5328.
17 J. Wei, L. Liao, Y. Xiao, P. Zhang and Y. Shi, *J. Environ. Sci.*, 2010, **22**, 1558–1563.
18 X. Xu, J. M. Andresen, C. Song, B. G. Miller and A. W. Scaroni, *ACS Div. Fuel Chem. Prepr.*, 2002, **47**, 67–68.
19 M. R. Mello, D. Phanon, G. Q. Silveira, P. L. Llewellyn and C. M. Ronconi, *Microporous Mesoporous Mater.*, 2011, **143**, 174–179.
20 A. Heydari-Gorji, Y. Yang and A. Sayari, *Energy and Fuels*, 2011, **25**, 4206–4210.
21 W. Chaikittisilp, H. J. Kim and C. W. Jones, *Energy and Fuels*, 2011, **25**, 5528–5537.
22 S. Komarneni, X. Yan, K. Qiao, Y. Zhang, Z. Yan, X. Li and Z. Zhang, *J. Hazard. Mater.*, 2011, **192**, 1505–1508.
23 C. Chen and W. S. Ahn, *Chem. Eng. J.*, 2011, **166**, 646–651.
24 D. Wang, C. Sentorun-Shalaby, X. Ma and C. Song, *Energy and Fuels*, 2011, **25**, 456–458.
25 Z. Chen, S. Deng, H. Wei, B. Wang, J. Huang and G. Yu, *ACS Appl. Mater. Interfaces*, 2013, **5**, 6937–6945.
26 E. S. Sanz-pérez, L. Rodríguez-jardón, A. Arencibia, R. Sanz, M. Iglesias and E. M. Maya, *J. CO2 Util.*, 2019, **30**, 183–192.
27 Z. Y. Sui, Y. Cui, J. H. Zhu and B. H. Han, *ACS Appl. Mater. Interfaces*, 2013, **5**, 9172–9179.
28 A. Kulur, J. A. A. Gibson, S. Brandani, A. V. Gromov, E. Mangano and E. E. B. Campbell, *Sustain. Energy Fuels*, 2018, **2**, 1630–1640.
29 C. Gebald, J. A. Wurzbacher, P. Tingaut, T. Zimmermann and A. Steinfeld, *Environ. Sci. Technol.*, 2011, **45**, 9101–9108.
30 M. A. Sakwa-Novak, C.-J. Yoo, S. Tan, F. Rashidi and C. W. Jones, *ChemSusChem*, 2016, **9**, 1859–1868.
31 P. M. Eisenberger, *US 9,227,153 B2*, 2016.
32 C. Chen, S.-T. Yang, W.-S. Ahn and R. Ryoo, *Chem. Commun.*, 2009, 3627–3629.
33 A. R. Sujan, S. H. Pang, G. Zhu, C. W. Jones and R. P. Lively, *ACS Sustain. Chem. Eng.*, 2019, **7**, 5264–5273.
34 F. Yin, L. Zhuang, X. Luo and S. Chen, *Appl. Surf. Sci.*, 2018, **434**, 514–521.
35 Y. Chen, G. Shao, Y. Kong, X. Shen and S. Cui, *Chem. Eng. J.*, 2017, **322**, 1–9.
36 J. Zhu, L. Wu, Z. Bu, S. Jie and B. G. Li, *Ind. Eng. Chem. Res.*, 2017, **56**, 10155–10163.
37 S. K. Kundu and A. Bhaumik, *ACS Sustain. Chem. Eng.*, 2016, **4**, 3697–3703.
38 Y. Zhu, H. Long and W. Zhang, *Chem. Mater.*, 2013, **25**, 1630–1635.
39 M. R. Liebl and J. Senker, *Chem. Mater.*, 2013, **25**, 970–980.
40 K. S. Hwang, H. Y. Park, J. H. Kim and J. Y. Lee, *Korean J. Chem. Eng.*, 2018, **35**, 798–804.
41 X. Xu, B. Pejcic, C. Heath and C. D. Wood, *J. Mater. Chem. A*, 2018, **6**, 21468–21474.
42 Y. Wang, D. Kong, W. Shi, B. Liu, G. J. Sim, Q. Ge and H. Y. Yang, *Adv. Energy Mater.*, 2016, **6**, 1–9.
43 W. Chen, Y. X. Huang, D. B. Li, H. Q. Yu and L. Yan, *RSC Adv.*, 2014, **4**, 21619–21624.
44 C. J. Gommes, S. Blacher, J. H. Dunsmuir and A. H. Tsou, *AIChE J.*, 2012, **55**, 2000–2012.
45 M. Chau, K. J. De France, B. Kopera, V. R. Machado, S. Rosenfeldt, L. Reyes, K. J. W. Chan, S. Förster, E. D. Cranston, T. Hoare and E. Kumacheva, *Chem. Mater.*, 2016, **28**, 3406–3415.
46 S. Chatterjee, S. Sen Gupta and G. Kumaraswamy, *Chem. Mater.*, 2016, **28**, 1823–1831.
47 L. Shechter and J. Wynstra, *Industial Eng. Chem.*, 1956, **48**, 86–93.

This journal is © The Royal Society of Chemistry 20xx

Please do not adjust margins

48 L. Shechter, J. Wynstra and R. P. Kurkjy, *Ind. Eng. Chem.*, 1956, **48**, 94–97.
49 X. Wang, V. Schwartz, J. C. Clark, X. Ma, S. H. Overbury, X. Xu and C. Song, *J. Phys. Chem. C*, 2009, **113**, 7260–7268.
50 M. A. Sakwa-Novak, S. Tan and C. W. Jones, *ACS Appl. Mater. Interfaces*, 2015, **7**, 24748–24759.
51 D. K. Wang, S. Varanasi, P. M. Fredericks, D. J. T. Hill, A. L. Symons, A. K. Whittaker and F. Rasoul, *J. Polym. Sci. Part A Polym. Chem.*, 2013, **51**, 5163–5176.
52 K. Isa, M. Aghazadeh and T. Doroudi, *Anal. Bioanal. Electrochem*, 2016, **8**, 604–614.
53 S. T. Navale, G. D. Khuspe, M. A. Chougule and V. B. Patil, *RSC Adv.*, 2014, **4**, 27998–28004.
54 C. Chen, C. J. Wang, H. Xu and H. Q. Dai, *BioResources*, 2017, **12**, 6378–6391.
55 Y. Wu, C. Liu, X. Zhao and J. Xiang, *J Polym Res*, 2008, **15**, 181–185.
56 K. Shameli, M. Mahdavi, P. Shabanzadeh, S. D. Jazayeri, M. Bin Ahmad, S. Sedaghat, Y. Abdollahi and H. Jahangirian, *Int. J. Mol. Sci.*, 2012, **13**, 6639–6650.
57 H. Zhang, I. Hussain, M. Brust, M. F. Butler, S. P. Rannard and A. I. Cooper, *Nat. Mater.*, 2005, **4**, 787–793.
58 M. Bailey and J. Hallett, *J. Atmos. Sci.*, 2004, **61**, 514–544.
59 *J. Appl. Phys.*, 1983, **54**, 2677–2682.
60 T. Waschkies, R. Oberacker and M. J. Hoffmann, *Acta Mater.*, 2011, **59**, 5135–5145.
61 T. Waschkies, R. Oberacker and M. J. Hoffmann, *J. Am. Ceram. Soc.*, 2009, **84**, 79–84.
62 Y. Wang, M. D. Gawryla and D. A. Schiraldi, *J. Appl. Polym. Sci.*, 2013, **129**, 1637–1641.
63 S. Deville, E. Saiz and A. P. Tomsia, *Acta Mater.*, 2007, **55**, 1965–1974.
64 E. S. Sanz-Pérez, A. Arencibia, G. Calleja and R. Sanz, *Microporous Mesoporous Mater.*, 2018, **260**, 235–244.
65 X. Yan, L. Zhang, Y. Zhang, K. Qiao, Z. Yan and S. Komarneni, *Chem. Eng. J.*, 2011, **168**, 918–924.
66 A. Heydari-Gorji, Y. Yang and A. Sayari, *Energy & Fuels*, 2011, **25**, 4206–4210.
67 A. Heydari-Gorji, Y. Belmabkhout and A. Sayari, *Langmuir*, 2011, **27**, 12411–12416.
68 G. P. Knowles, J. V. Graham, S. W. Delaney and A. L. Chaffee, *Fuel Process. Technol.*, 2005, **86**, 1435–1448.
69 K. Li, J. D. Kress and D. S. Mebane, *J. Phys. Chem. C*, 2016, **120**, 23683–23691.
70 A. Danon, P. C. Stair and E. Weitz, *J. Phys. Chem. C*, 2011, **115**, 11540–11549.
71 G. S. Foo, J. J. Lee, C.-H. Chen, S. E. Hayes, C. Sievers and C. W. Jones, *ChemSusChem*, 2017, **10**, 266–276.
72 J. J. Lee, C.-H. Chen, D. Shimon, S. E. Hayes, C. Sievers and C. W. Jones, *J. Phys. Chem. C*, 2017, **121**, 23480–23487.
73 C.-H. Chen, D. Shimon, J. J. Lee, F. Mentink-Vigier, I. Hung, C. Sievers, C. W. Jones and S. E. Hayes, *J. Am. Chem. Soc.*, 2018, **140**, 8648–8651.
74 M. Caplow, 1968, 6795–6803.
75 T. L. Donaldson and Y. N. Nguyen, *Ind. Eng. Chem. Fundam.*, 1980, **19**, 260–266.
76 A. Sayari, A. Heydari-Gorji and Y. Yang, *J. Am. Chem. Soc.*, 2012, **134**, 13834–13842.
77 A. Heydari-gorji and A. Sayari, *Ind. Eng. Chem. Res.*, 2012, **51**, 6887–6894.
78 W. Choi, K. Min, C. Kim, Y. S. Ko, J. W. Jeon, H. Seo, Y. K. Park and M. Choi, *Nat. Commun.*, 2016, **7**, 12640.
79 A. Goeppert, H. Zhang, R. Sen, H. Dang, S. G. Prakash and G. K. S. Prakash, *ChemSusChem*, , DOI:10.1002/cssc.201802978.

Please do not adjust margins

TOC Graphic

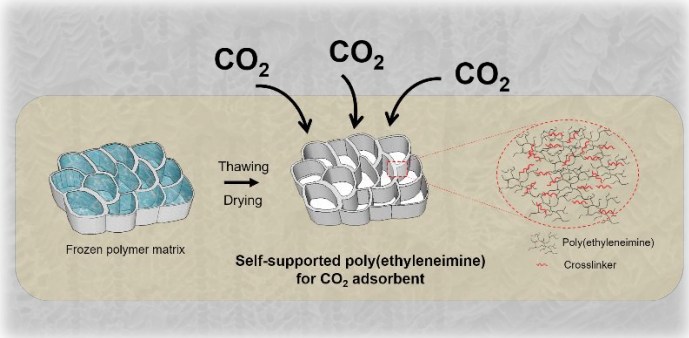

A family of self-supported, cross-linked PEI materials is demonstrated as promising CO_2 adsorbents, displaying (i) good CO_2 capacity (ii) rapid uptake kinetics, and (iii) good stability relative to conventional supported amine adsorbents.